Visualizing Nanoscale Dynamics with Time-resolved Electron Microscopy

Jonathan M. Voss, Pavel K. Olshin, Marcel Drabbels, and Ulrich J. Lorenz*

Abstract: The large number of interactions in nanoscale systems leads to the emergence of complex behavior. Understanding such complexity requires atomic-resolution observations with a time resolution that is high enough to match the characteristic timescale of the system. Our laboratory's method of choice is time-resolved electron microscopy. In particular, we are interested in the development of novel methods and instrumentation for high-speed observations with atomic resolution. Here, we present an overview of the activities in our laboratory.

Keywords: *In situ* electron microscopy · Nanoparticles · Nanoscale dynamics · Proteins · Time-resolved electron microscopy

Jonathan Voss obtained a B.S. in Chemistry and a B.S. in Forensic Science from the University of New Haven. During his PhD at the University of Wisconsin–Madison, he used mass spectrometry and laser spectroscopy to investigate solvation effects and catalytic reaction intermediates. Since 2018, he has been a postdoctoral scholar in the group of Ulrich Lorenz at EPFL, where he has worked on developing a novel approach to time-resolved cryo-electron microscopy that affords microsecond time resolution.

Pavel Olshin received a B.S. and M.S. in Laser Chemistry from Saint Petersburg State University. During his PhD in the group of Ulrich Lorenz at EPFL, he developed new instrumentation for time-resolved electron microscopy and applied it to study a range of fast, nanoscale dynamics. Since 2021, he has been a postdoctoral researcher in the group of Oh-Hoon Kwon at the Ulsan National Institute of Science and Technology, where he uses time-resolved electron microscopy to study cathodoluminescence phenomena.

Marcel Drabbels obtained a PhD in Physics from the University of Nijmegen in 1993. After postdoctoral stays at the University of California Santa Barbara and the FOM Institute for Atomic and Molecular Physics, he was awarded a fellowship by the Royal Netherlands Academy of Arts and Sciences in 1997 to start a research program at the Free University of Amsterdam. He moved to EPFL a year later, where as an independent senior scientist, he established a line of research on the spectroscopy and dynamics of nanoscale systems. He joined the Laboratory of Molecular Nanodynamics at EPFL in 2017, where he is currently Adjunct Professor.

Ulrich Lorenz obtained a Diploma in Chemistry from the University of Würzburg and a PhD from EPFL. His doctoral research revolved around the spectroscopy and dynamics of cryogenic molecular ions in the gas phase. He became interested in time-resolved electron microscopy during his postdoc in the group of Ahmed Zewail at Caltech. Since 2016, he has been an Assistant Professor in Chemistry at EPFL, where his work has been supported by an SNSF Professorship as well as an ERC Starting Grant. His group uses time-resolved electron microscopy to observe fast, nanoscale phenomena and has a particular emphasis on the development of new methods.

1. Introduction

Structure and dynamics are the most fundamental concepts of chemistry, and the nature of the chemical bond[1] and its dynamics[2] ultimately determine the properties of molecules. However, despite our understanding of these concepts, the multitude of interactions present in large systems frequently leads to an overwhelming complexity.[3] Proteins exemplify the emergence of complex behavior at the nanoscale. Given the huge number of degrees of freedom present in these large molecular systems, predicting their behavior has remained a daunting challenge.[4] Understanding the function of proteins and the dynamics of complex systems in general thus requires experimental approaches that allow observations with atomic spatial resolution as well as a temporal resolution that matches the characteristic timescale of the system.

Our laboratory's method of choice for studying the behavior of complex nanoscale systems is electron microscopy, which in recent years has undergone several revolutions. A number of technical innovations have improved the performance and resolution capabilities of electron microscopes, among them field emission guns, which generate very bright and coherent electron beams and thus fundamentally improve how much information can be obtained.[5–9] The introduction of novel electron cameras has enabled observations with higher frame rates and with improved sensitivity.[10,11] This has also accelerated a true revolution in cryo-electron microscopy (cryo-EM),[12–14] which now appears set to become the preferred method in structural biology.[15] *In situ* electron microscopy has enabled observations of processes in liquid phase[16] as well as processes occurring in response to mechanical,[17] thermal,[18] electrical,[19,20] or optical[21] excitation.

*Correspondence: Prof. U. J. Lorenz,
E-mail: ulrich.lorenz@epfl.ch, Ecole Polytechnique Fédérale de Lausanne (EPFL),
Laboratory of Molecular Nanodynamics, CH-1015 Lausanne, Switzerland

Given the small dimensions of nanoscale samples, some of these processes occur on timescales much shorter than the time resolution of even the fastest electron cameras. Time-resolved electron microscopy has enabled observations on such short timescales by capturing specimen dynamics with short electron pulses.[22–25]

It is truly an exciting time to do electron microscopy – particularly because the recent introduction of such a wide range of new technologies has created a large potential to further advance the boundaries of what can be observed with an electron microscope. Our laboratory has a particular interest in the development of novel methods and instrumentation for high-speed observations with atomic resolution. In this account, we highlight recent innovations we have introduced to enable such observations of complex nanoscale systems. Section 2 introduces fundamental concepts of *in situ* and time-resolved electron microscopy and describes the time-resolved electron microscopes that we have developed in our laboratory. Section 3 illustrates an application of our instrument to the *in situ* observation of the interaction of plasmonic nanoparticles with laser light. Direct observations allow us to elucidate the long-debated mechanism of the femtosecond laser-induced fragmentation of gold nanoparticles. In Section 4, we turn our attention to the challenge of imaging fast dynamics at atomic resolution. We present an approach for generating intense, high-brightness electron pulses that enable atomic-resolution observations on the microsecond timescale. As an illustration, we show that such pulses can be used to capture the thermally-induced transformations of perovskite nanocrystals on the microsecond timescale. Finally, in Section 5, we describe a new approach to microsecond time-resolved cryo-EM that we have developed in our laboratory. By enabling atomically-resolved observations of the dynamics of proteins, it promises to fundamentally advance our knowledge of protein function.

2. Development of a Time-resolved Transmission Electron Microscope with a Schottky Emitter

Time-resolved electron microscopy is a comparably young field, with the instrumentation still undergoing active development. The first step in establishing our laboratory therefore required us to modify a conventional transmission electron microscope for time-resolved experiments. This also gave us the opportunity to tailor the instrument specifically to our vision. In particular, we decided to modify a microscope with a so-called Schottky field emission gun, a type of electron source that delivers one of the brightest electron beams.[5–9] Since the beam brightness ultimately determines how much information can be collected in a given amount of time, using a high-brightness source is particularly beneficial for time-resolved experiments. As described in Section 4, this is also crucial for the generation of intense, high-brightness electron pulses for atomic-resolution imaging. Our laboratory has modified two such transmission electron microscopes, and we are currently setting up a third. In this section, we will briefly outline the operating principle, which lays the foundation for the following sections.

Fig. 1a illustrates the operating principle of the modified JEOL 2200FS transmission electron microscope in our laboratory.[26] In conventional operation, electrons are continuously emitted from the Schottky emitter and accelerated to relativistic speeds. After the electrons interact with the sample, magnetic lenses are used to form an image or diffraction pattern, which is then recorded with the electron camera. An energy filter located in the column of the instrument serves to either select or discard electrons that have undergone inelastic interactions, so as to provide additional information about the sample or improve the image resolution.

In order to study dynamic processes, the sample is irradiated *in situ* with a laser pulse (Fig. 1a, red), which enters the microscope from the side and is reflected onto the sample by means of a mirror that we have installed above the upper pole piece of the object
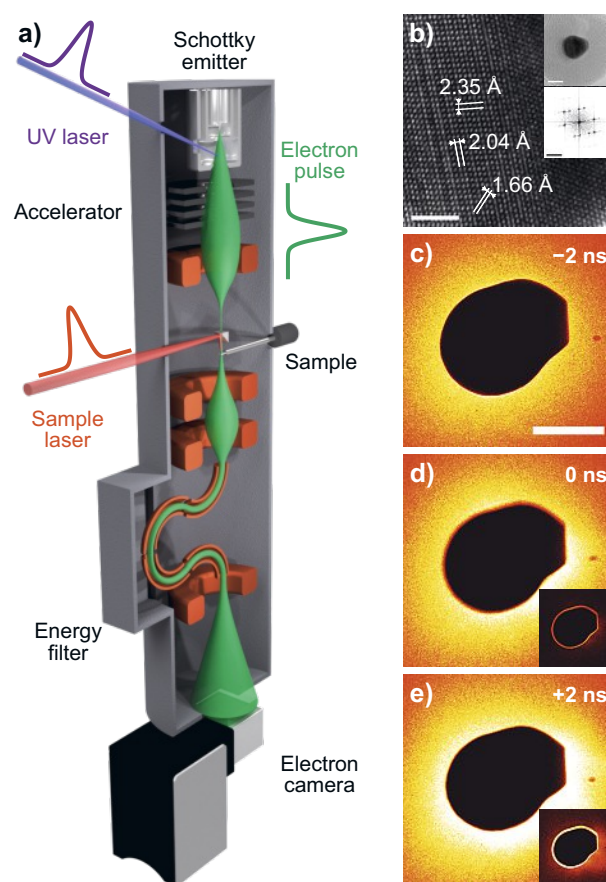

Fig. 1. Operating principle and characterization of a time-resolved electron microscope. (a) Sketch of the JEOL 2200FS transmission electron microscope that we have modified for time-resolved experiments. The sample laser (red) is used to initiate specimen dynamics. In a typical *in situ* experiment, the evolution of the sample is then filmed with the electron camera. Even shorter timescales can be accessed by probing the dynamics with short electron pulses (green), which are generated by illuminating the Schottky emitter with a UV laser pulse of nanosecond or femtosecond duration (purple). (b) High-resolution image of the core of a silica-coated gold nanoparticle, demonstrating the spatial resolution capabilities of our instrument. The entire nanoparticle is depicted in the top inset, with the diffractogram shown in the bottom inset. Scale bar, 2 nm, as well as 10 nm and 5 nm⁻¹ in the insets. (c–e) Characterization of the temporal resolution in a stroboscopic experiment with nanosecond electron pulses. Under irradiation with femtosecond laser pulses, a gold nanoparticle emits a cloud of electrons, which causes the particle outline to blur at positive time delays. The insets show difference micrographs, which are obtained by subtracting the micrograph recorded at -2 ns. From this experiment, we determine an electron pulse duration of 1.3 ns. Scale bar, 100 nm. (Adapted from ref. [26].)

lens. In a typical *in situ* experiment, the structural evolution of the sample in response to laser excitation is then filmed with the electron camera. The speed of such observations is limited by the frame rate of the camera, which is on the order of milliseconds. In order to access even shorter timescales, we capture snapshots of the sample with short electron pulses of nanosecond or even femtosecond duration instead of observing it with a continuous electron beam. Such electron pulses (Fig. 1a, green) are created with the photoelectric effect by illuminating the emitter with a short UV laser pulse (Fig. 1a, purple), while the continuous electron emission is suppressed.

The high-resolution capabilities of our modified microscope are illustrated in Fig. 1b, which shows the core of a silica-coated gold nanoparticle (top inset, 20 nm thick shell and 20 nm diameter core), as imaged with a continuous electron beam.[26] The lattice fringes visible in the image result from the diffraction of

the electrons at the atomic columns of the particle, with the fringe spacings corresponding to the interatomic distances of gold (see diffractogram in the bottom inset). This demonstrates that the modifications of our microscope have preserved its atomic-resolution capabilities.

Fig. 1c–e illustrates an experiment to characterize the temporal resolution of our instrument when imaging a sample stroboscopically with nanosecond electron pulses. The experiment makes use of the fact that under irradiation with an intense femtosecond laser pulse, a gold nanoparticle emits a cloud of electrons. At negative times, *i.e.* when the nanosecond electron pulse precedes the femtosecond laser pulse, the border of the nanoparticle appears sharp (Fig. 1c). In contrast, when the two pulses arrive at the sample simultaneously, the particle outline broadens (Fig. 1d), since the nanosecond electron pulse is deflected by the cloud of emitted electrons. This blurring is even more pronounced at positive times (Fig. 1e). It is highlighted by the difference images displayed in the insets, which are obtained by subtracting the micrograph recorded at negative time. This experiment allows us to determine our electron pulses have a duration of 1.3 ns. In order to probe dynamics that unfold on even shorter timescales, we generate femtosecond electron pulses. Finally, Section 4 describes the generation of intense, high-brightness electron pulses of microsecond duration that allow us to capture atomic-resolution snapshots of irreversible processes.

3. *In situ* Observations of the Laser-induced Fragmentation of Plasmonic Nanoparticles

In one of the first studies we undertook, we used the *in situ* observation capabilities of our microscope to elucidate the mechanism of the femtosecond laser-induced fragmentation of plasmonic nanoparticles, which had long been debated.[27–29] Because of their strong and tunable plasmonic absorption, gold nanoparticles have found a wide range of applications, including in chemical and biological sensors,[30,31] in catalysts,[32] for cancer treatment,[33,34] and in solar cells.[35,36] Laser reshaping and fragmentation has long been used to tune the optical properties of gold nanoparticles.[37,38]

For example, ultrafast laser pulses can be used to fragment gold nanoparticles dispersed in water and generate fragments of 2–4 nm diameter, a size range that is otherwise difficult to synthesize.[27,37,39,40] However, in the absence of direct observations, the mechanism of this process has remained a matter of debate.[27–29] Both a thermal explosion[27,41] as well as a Coulomb explosion[39] have been proposed to account for the observed fragmentation behavior. Moreover, near-field ablation[42] and shockwave-mediated disintegration[43] have been considered. Using the microscope that we have developed in our lab, we have been able for the first time to directly observe the fragmentation process, which has allowed us to elucidate the underlying mechanism.

We initially characterized the fragmentation mechanism of gold nanoparticles enclosed in a silica shell,[21] a more tractable model system that shares many similarities with the fragmentation process in water. Fig. 2a shows a micrograph of a typical silica-coated gold nanoparticle with a 20 nm diameter core and a 20 nm thick shell. Upon irradiation with 515 nm femtosecond laser pulses at 20 kHz repetition rate, the gold core emits a small particle (Fig. 2b). Under continued irradiation, further fragments are ejected (Fig. 2c,d), each comprising approximately 30–200 atoms. These fragments finally coalesce into a larger mass (Fig. 2e), which continues to grow (Fig. 2f,g), until it reaches a similar size as the original core and begins to emit fragments itself (Fig. 2h). Fragmentation clearly proceeds through the stepwise ejection of progeny particles, an observation that contradicts mechanisms that invoke an explosion into a large number of fragments. Curiously, the ejection of fragments is highly directional and occurs preferentially along the laser polarization axis (double-headed arrow in Fig. 2a). Moreover, fragmentation appears to involve the melting of the gold core, whose shape fluctuates under laser irradiation.

Our observations suggest that the fragmentation mechanism involves the Coulomb fission of the ionized, liquid gold core (Fig. 2i–l). During ultrafast laser irradiation (240 fs), electrons are emitted in the direction of the laser polarization, producing an anisotropic buildup of negative charge in the silica shell (Fig. 2i).

Fragmentation of gold nanoparticles in a silica shell
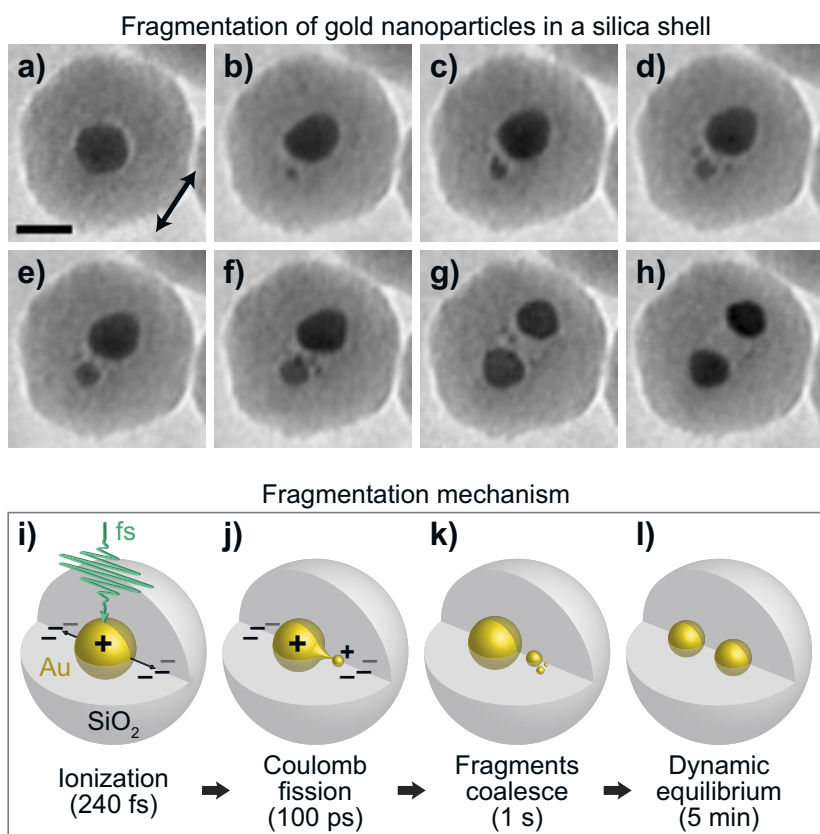

Fragmentation mechanism

Fig. 2. Femtosecond laser-induced fragmentation of a silica-coated gold nanoparticle. (a–h) A typical fragmentation process. The gold core ejects fragments in a stepwise manner, with ejection occurring predominantly in the direction of the laser polarization (double-headed arrow). The fragments subsequently coalesce into a second core. (i–l) Proposed fragmentation mechanism. (i) The femtosecond laser ionizes the core. Electrons are emitted in the direction of the laser polarization and become trapped in the silica shell. (j) The gold core melts and undergoes Coulomb fission by ejecting a highly charged progeny droplet in the direction of the patches of negative charge in the silica shell. (k) Progeny droplets accumulate and fuse together to form a second core. (l) A dynamic equilibrium is established as the cores exchange droplets through fission. (Adapted from ref. [21].)

The gold core subsequently melts as electron–phonon coupling heats up the lattice. The resulting ionized liquid gold droplet then undergoes Coulomb fission by emitting a highly-charged progeny droplet towards the negatively charged region of the silica shell, a process which can be estimated to take about 100 ps[21] (Fig. 2j). Continued laser irradiation causes further progeny particles to be ejected, which then coalesce into a second core (Fig. 2k). As this second core continues to grow, it begins to undergo fission itself, and a dynamic equilibrium is slowly established in which the two cores exchange progeny particles (Fig. 2l).

We subsequently studied the fragmentation of gold nanoparticles dispersed in water, showing that the mechanism similarly involves Coulomb fission, which is accompanied by other solution-mediated processes.[44] As illustrated in Fig. 3a, we enclose a suspension of gold nanoparticles in a microchip-based liquid cell,[45] which prevents evaporation of the liquid in the vacuum of the microscope. Fig. 3b–f shows a typical fragmentation process that we observe under irradiation with 515 nm femtosecond laser pulses at 10 kHz repetition rate. The two particles in Fig. 3b can be seen to melt and begin to eject several small fragments (Fig. 3c). Under continued irradiation, the fragment particles grow in size (Fig. 3d) and begin to fragment themselves (Fig. 3e,f). Progeny particles are ejected in a stepwise manner, which is reminiscent of the fragmentation of the core-shell particles and therefore suggests that the underlying mechanism is Coulomb fission. Unlike for the core-shell particles, however, ejection does not occur in a preferred direction.

Based on our observations, we proposed the following fragmentation mechanism (Fig. 3g–j). Irradiation with a femtosecond laser (200 fs) ionizes the nanoparticle and ejects electrons in the direction of the laser polarization (Fig. 3g). The solvated electrons quickly diffuse away, so that an isotropic charge distribution is established in the water before the next laser pulse arrives 100 µs later. Continued laser irradiation ionizes the particle until it reaches the stability limit. As it is melted by a laser pulse, it undergoes Coulomb fission by emitting a charged progeny droplet in a random direction (Fig. 3h). Under continued laser irradiation, complex fragmentation patterns are created, and progeny particles undergo fission themselves (Fig. 3i). Finally, a state of flux is reached, in which repeated cycles of fission and fusion as well as solution-mediated etching and growth processes continuously reshuffle mass between the fragments (Fig. 3j).
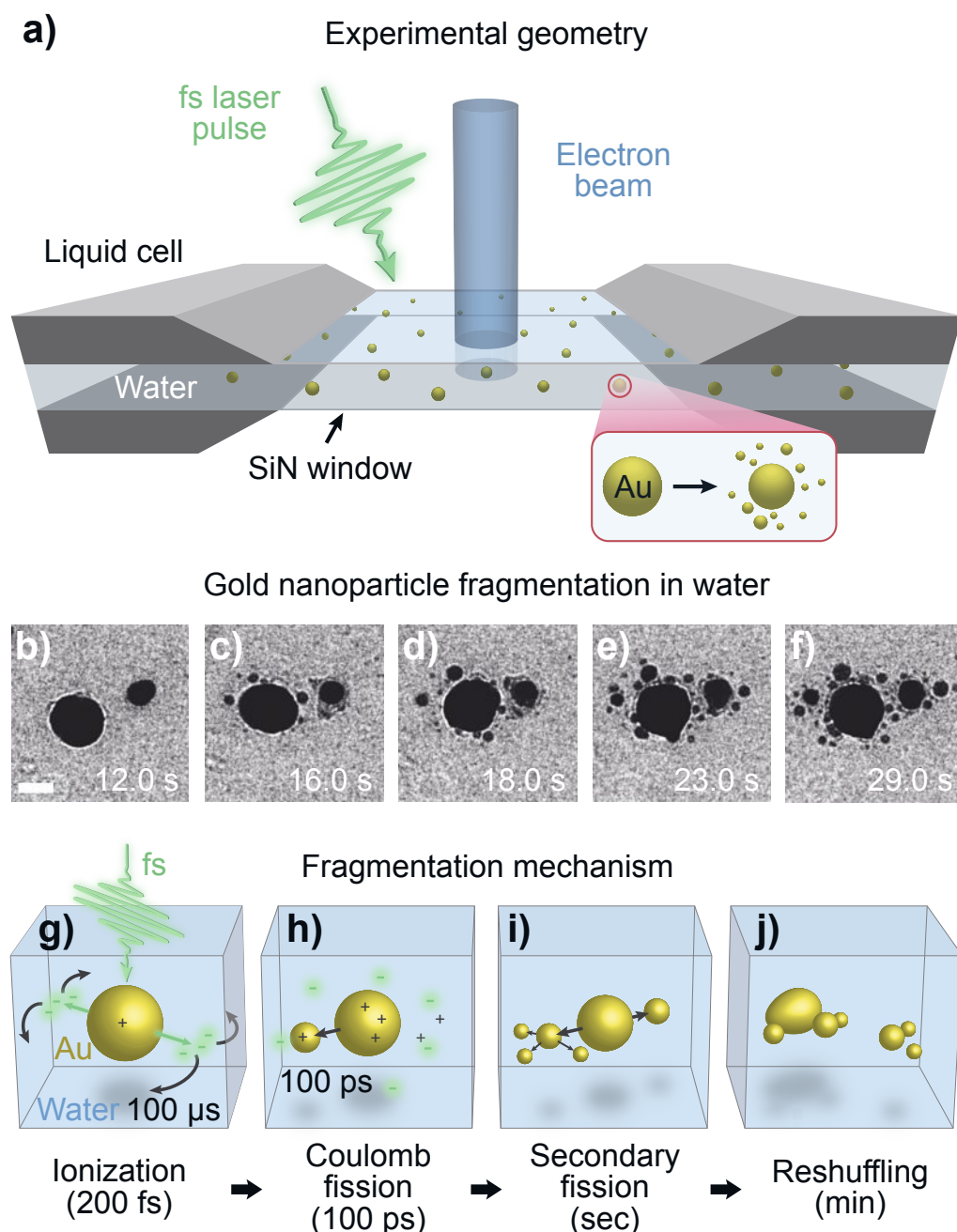

Fig. 3. Femtosecond laser-induced fragmentation of gold nanoparticles in water. (a) Gold nanoparticles suspended in water are enclosed in a liquid cell and are irradiated with femtosecond laser pulses, while the fragmentation process is observed with the electron beam. (b–f) A typical fragmentation process. Under laser irradiation, the gold nanoparticles melt and eject fragments in a stepwise fashion without any preferred direction. The ejected particles grow in size and undergo fragmentation themselves. (g–j) Proposed fragmentation mechanism. (g) The laser ionizes the particle, and electrons are emitted along the direction of the laser polarization. The solvated electrons quickly diffuse away, so that an isotropic charge distribution is established in the water. (h) Under continued laser irradiation, the particle is ionized to the stability limit and undergoes Coulomb fission, emitting a fragment in a random direction. (i) Progeny particles grow and undergo fission themselves. (j) Cycles of fission and fusion as well as solution-mediated etching and growth processes create complex, fluctuating fragmentation patterns. (Adapted from ref. [44].)

Our experiments provide the most direct evidence to date of the fragmentation mechanism of plasmonic nanoparticles under femtosecond laser irradiation, highlighting the importance of the direct observation of fast, nanoscale processes. Moreover, they open up new avenues to elucidate the light-driven shape transformations of plasmonic nanoparticles.[46,47]

4. Atomic-resolution Imaging with Intense, High-brightness Electron Pulses

The time resolution of the *in situ* experiments presented in Section 3 is limited by the frame rate of the camera, which is typically on the order of milliseconds. As discussed in Section 2, a much higher time resolution can be obtained by imaging with short electron pulses. However, the increased temporal resolution has generally come at the expense of the available spatial resolution, so that atomic-resolution imaging with short electron pulses has largely remained elusive. For example, while it has been suggested that it should be possible to image protein dynamics at atomic resolution with single electron pulses,[48,49] the currently achievable spatial resolution of such single-shot experiments is limited to several nanometers. The difficulty here lies in generating electron pulses that are intense enough to capture a sufficient amount of information, but also coherent enough to record atomic-resolution images. This is particularly true in the study of irreversible processes, where the entire information has to be captured with just a single electron pulse.

We have developed a new approach for creating intense, high-brightness electron pulses that enable atomic-resolution imaging with microsecond time resolution.[50,51] As illustrated in Fig. 4a, we accomplish this by irradiating the emitter tip with a microsecond laser pulse. This temporarily heats it far above its safe operating temperature and thus briefly boosts the emission current to an extreme value[50] that otherwise cannot be sustained without permanently damaging the emitter.[52,53] The laser-boosted electron beam is then chopped into pulses by means of an electrostatic deflector that we have added after the accelerator of the gun. This allows us to generate microsecond pulses of variable duration, and even pulses as short as 100 ns. As illustrated in Fig. 4b, the probe current (blue) rises rapidly when the emitter tip is irradiated with a 100 μs laser pulse (green). Chopping the boosted electron beam with the electrostatic deflector results in a 50 μs electron pulse (Fig. 4c). We can thus obtain electron pulses with almost four times the beam intensity and 1.7 times the brightness as with the filament operated under conventional conditions.

We have established that our laser-boosted electron pulses allow us to capture fast transformations of nanoparticles in a single shot and with atomic resolution.[51] Here, we study the structural
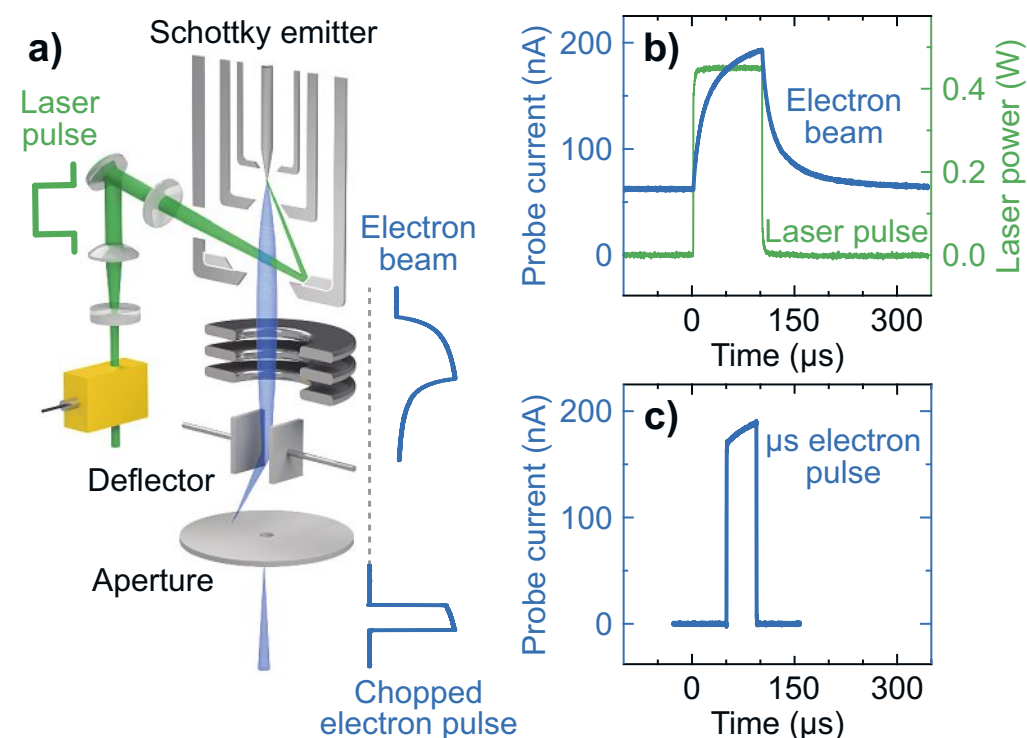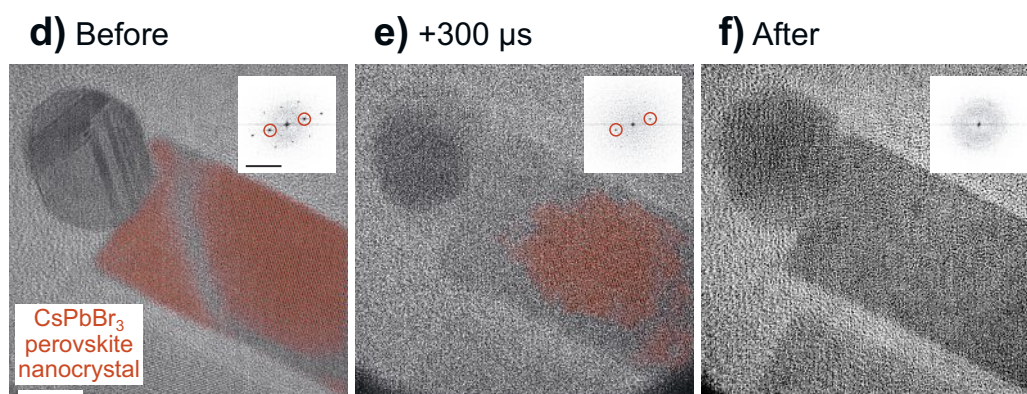

Fig. 4. Microsecond time-resolved imaging with intense, high-brightness electron pulses. (a) Illustration of the generation of intense, high-brightness electron pulses. The tip of the Schottky field emitter of the electron gun is heated to extreme temperatures with a microsecond laser pulse, thus boosting the emission current to near its maximum. An electrostatic deflector then chops the beam into microsecond pulses. (b) Irradiation of the emitter with a 100 μs laser pulse (green) boosts the probe current (blue). (c) A 50 μs electron pulse is obtained by chopping the boosted electron beam with the electrostatic deflector. (d–f) A $CsPbBr_3$ perovskite nanocrystal (d) is rendered amorphous when it is heated with a 500 μs laser pulse (f), as confirmed by the diffractogram of the crystal in the inset. A snapshot recorded with a 100 μs electron pulse after 300 μs of laser irradiation reveals that amorphization starts at the crystal surface (e). The red overlay highlights crystalline domains and is obtained by Fourier filtering the images with the reflections selected that are circled in the diffractogram in the inset. Scale bars, 10 nm and 5 nm⁻¹. (Adapted from ref. [51].)

transformations that CsPbBr$_3$ perovskite nanocrystals[54,55] undergo at elevated temperatures. The perovskite nanocrystal in Fig. 4d features a single crystalline domain highlighted in red. Heating the crystal with a 500 µs laser pulse renders it amorphous (Fig. 4f), a process that is known to be associated with the degradation of the performance of perovskite nanocrystals in optoelectronic applications and that hinders their use in high-power devices.[56] A snapshot taken during laser irradiation provides a subparticle picture of the mechanism involved, revealing that amorphization is initiated at the crystal boundaries and propagates inward (Fig. 4e). Crucially, this information can only be extracted because the snapshot features atomic resolution. For comparison, single-shot experiments had previously only reached a resolution of several nanometers.[49] Our intense, highly coherent electron pulses open up a new regime for atomic-resolution imaging on microsecond timescales that has so far largely remained unexplored. Similarly, our electron pulses greatly benefit high-resolution diffraction experiments on these timescales, as we have begun to explore.

5. Observing Protein Dynamics with Microsecond Time-resolved Cryo-EM

Proteins are a prominent example of the emergence of complex behavior in nanoscale systems and illustrate why we need to develop novel approaches for high-speed, atomic-resolution observations if we want to understand this complexity. Proteins provide the machinery of life and are involved in harvesting energy from the environment, sensing stimuli, metabolizing nutrients, and maintaining homeostasis. As nanoscale machines that carry out tasks, proteins are inherently dynamic systems. Yet, much of our knowledge about protein function still derives from static structures.[57–60] In the absence of real-time observations, however, our understanding of proteins must remain fundamentally incomplete.[61]

Observing proteins in action requires not only atomic spatial resolution, but also a temporal resolution that matches the fast motions of proteins, a challenge that has largely remained beyond the reach of existing methods in structural biology.[61] The dynamics associated with the activity of a protein frequently involve domain motions that occur on a timescale of microseconds to milliseconds.[62] Among the available atomic-resolution techniques, NMR spectroscopy is too slow to access such short timescales.[61] Ultrafast X-ray crystallography[63] has enabled the observation of photoinduced protein dynamics,[64,65] but requires a crystalline sample, which notably impedes any large-amplitude motions.[61] This is not the case for cryo-EM, which images proteins in the frozen hydrated state.[12,13] However, the time resolution of traditional time-resolved cryo-EM has been limited to a few milliseconds.[66–69] It has thus remained impossible to directly observe the domain motions of proteins that occur on the microsecond timescale.

In our lab, we have developed a novel approach to time-resolved cryo-EM that improves its temporal resolution by a factor of 1000. It thus enables atomic-resolution observations of protein dynamics on the microsecond timescale and therefore promises to fundamentally change what we can know about protein function.[70–72] Fig. 5a–e illustrates our experimental approach, which is very much orthogonal to existing techniques. It uses a laser to rapidly melt a cryo sample, in which proteins are embedded in a thin layer of vitreous ice (Fig. 5a). Once in their native liquid environment at room temperature (Fig. 5b), the embedded particles are subjected to an external stimulus that induces dynamics (Fig. 5c). For example, a second laser pulse can be used to dissociate a caged compound and thus induce a rapid change in the chemical environment of the protein.[73,74] While these dynamics unfold, the heating laser is switched off at a well-defined point in time, which causes the sample to rapidly cool and revitrify. Particles are thus trapped in their transient configurations (Fig. 5d), which can subsequently be imaged with established cryo-EM techniques, so as to obtain their three-dimensional structure (Fig. 5e).
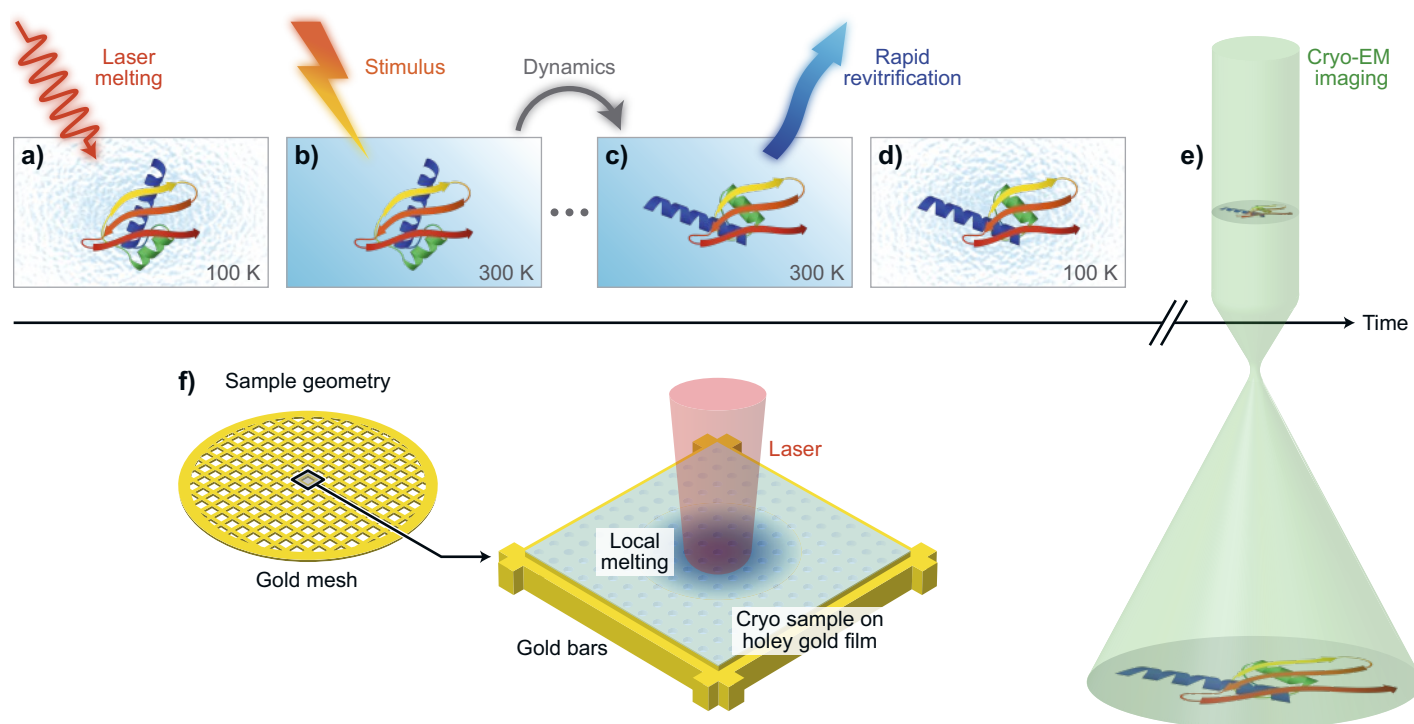

Fig. 5. Experimental concept of microsecond time-resolved cryo-EM and sample geometry. (a) A cryo sample is melted *in situ* with a laser beam. (b) Once the sample is liquid and has reached room temperature, dynamics of the embedded particles are induced with an external stimulus. (c) As the particles undergo conformational changes, the heating laser is switched off, so that the sample rapidly cools and revitrifies. (d,e) The particles are trapped in their transient configurations and can be subsequently imaged with conventional cryo-EM techniques. (f) Sketch of the sample geometry. (Adapted from ref. [70].)

Fig. 5f illustrates a typical sample geometry used in our experiments. A thin cryo sample (approximately 100 nm thick) is suspended over a holey gold film[75] (50 nm thickness), which is supported by the gold mesh of a specimen grid. The sample is held at 100 K by means of a liquid nitrogen-cooled specimen holder. The heating laser beam (532 nm) is aligned to the center of a grid square, where it locally melts the cryo sample.

A proof-of-principle experiment demonstrates the viability of our approach, showing that we can melt a cryo sample and allow particle dynamics to occur in liquid phase, and that we can rapidly revitrify it after the end of the laser pulse, thus trapping the proteins in their transient states (Fig. 6).[71] We make use of the well-known fact that proteins incur electron beam damage during cryo imaging. It is commonly believed that the vitreous ice matrix counteracts this damage and preserves the protein structure by fixing fragments in place. However, melting the sample should allow the particles to unravel once they find themselves in a liquid environment. This is exactly what we observe in our experiment. We first image a conventional cryo sample of apoferritin by illuminating only the circular areas in the top left and bottom right with a dose of 5 electrons/Å^2 and 10 electrons/Å^2, respectively (Fig. 6a). We subsequently melt and revitrify the sample with a 15 µs laser pulse (Fig. 6b). We find that particles in the areas that have previously been exposed to the electron beam have disassembled and have been trapped in partially unraveled states (Fig. 6d,e). Disassembly becomes more pronounced with electron dose, so that for the particles exposed to 10 electrons/Å^2, only small fragments remain that barely offer any contrast (Fig. 6e). At the same time, particles that have not incurred any beam damage are left intact (Fig. 6c).

Three-dimensional reconstructions confirm that the melting and revitrification process leaves the protein structure intact, which is crucial for our method to be useful for time-resolved studies of protein dynamics.[72] Fig. 7a shows a typical micrograph of a conventional apoferritin cryo sample together with a single-particle reconstruction obtained on our instrument. At a resolution of 4.57 Å, we can resolve individual helices as well as some side-chain density. If we melt and revitrify the cryo sample, the visual appearance of the apoferritin particles is similar (Fig. 7b), with the reconstruction yielding a slightly higher resolution of 4.25 Å. Both structures are indistinguishable, allowing us to conclude that within the spatial resolution afforded by our instrument, the revitrification process does not alter the protein structure.

We have also established that our approach affords a time resolution of just a few microseconds.[70] The time resolution is determined by how quickly particles can be trapped in their transient configurations when the sample revitrifies, and thus by how fast the sample cools. We have used nanosecond time-resolved electron microscopy (Section 2) to measure the characteristic cooling time of the sample. In the absence of a film of vitreous ice, the holey gold film cools in just 3.6 µs. Simulations show that this timescale increases slightly in the presence of a cryo sample, but remains below 5 µs for a typical ice thickness. This short cooling time is a consequence of our experimental geometry, in which the laser warms up the sample only very locally, while the surroundings remain at cryogenic temperature. This allows for fast heat dissipation after the end of the laser pulse. With a temporal resolution of better than 5 µs, our approach is 1000 times faster than traditional time-resolved cryo-EM. Notably, this is fast enough to observe the domain motions of proteins that are typically associated with their function.

In conclusion, we have established a novel approach to time-resolved cryo-EM that enables high-resolution observations of protein dynamics with microsecond time resolution. It thus opens up new avenues to observe a wide range of protein dynamics that have previously remained inaccessible. Preliminary results indicate that we can obtain near-atomic resolution reconstructions by melting and revitrifying a sample in our instrument and then transferring it to a high-performance microscope for cryo imaging. Several strategies are available to impulsively excite dynamics. Photoactive systems can be triggered directly with a short laser pulse. Temperature jumps can be implemented simply by increasing the power of the melting laser, so that the sample reaches a higher temperature. Moreover, a range of biomimetic stimuli can be provided by releasing caged compounds through UV irradiation, such as ATP, ions, small peptides,[73,74] or redox active compounds.[77] Caged protons[78] and bases[79] can be used to induce pH jumps. Preliminary results show that these compounds can already be released with the sample still in the vitreous state, which significantly simplifies the experiment. Since the proteins are confined by the matrix of vitreous ice surrounding them, they cannot respond to a change in their chemical environment until
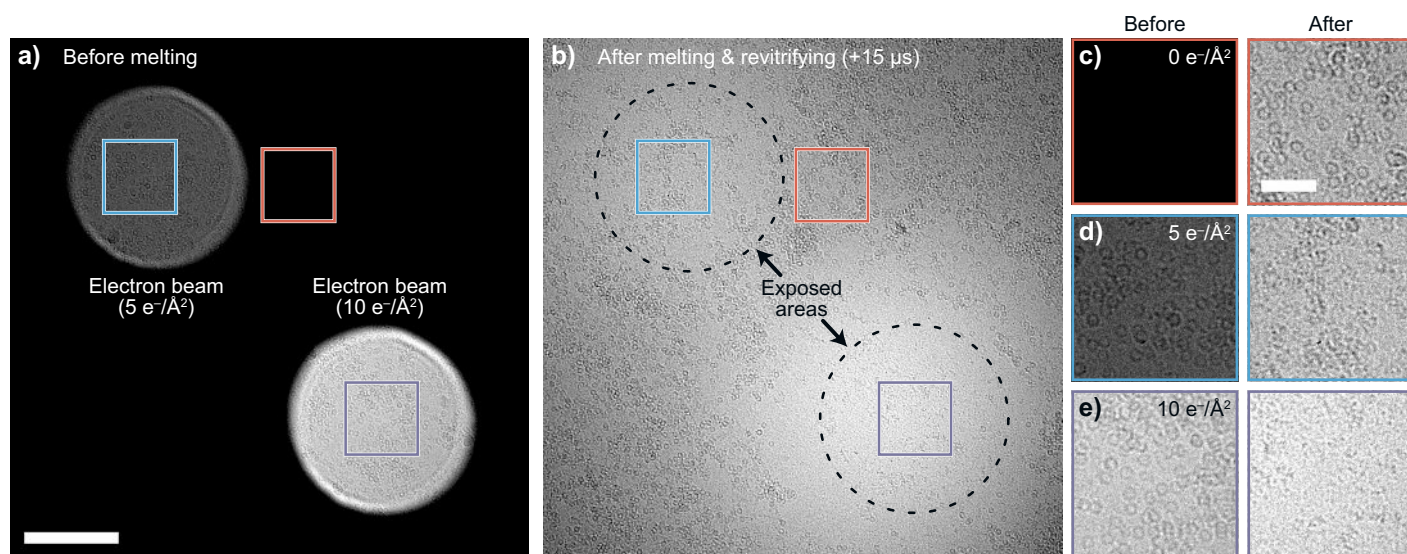

Fig. 6. Proof-of-principle demonstration of microsecond time-resolved cryo-EM. (a) Micrograph of a cryo sample of apoferritin. Only the circular areas in the top left and bottom right have been illuminated with an electron dose of 5 and 10 electrons/Å^2, respectively. Scale bar, 200 nm. (b) The sample is melted with a 15 µs laser pulse and revitrifies. (c) In areas that have not been illuminated with the electron beam prior to melting and revitrification, the particles have remained intact. Scale bar, 50 nm. (d,e) In contrast, particles that have incurred electron beam damage have unraveled while in liquid and have been trapped in partially disassembled configurations upon revitrification. (Adapted from ref. [71].)
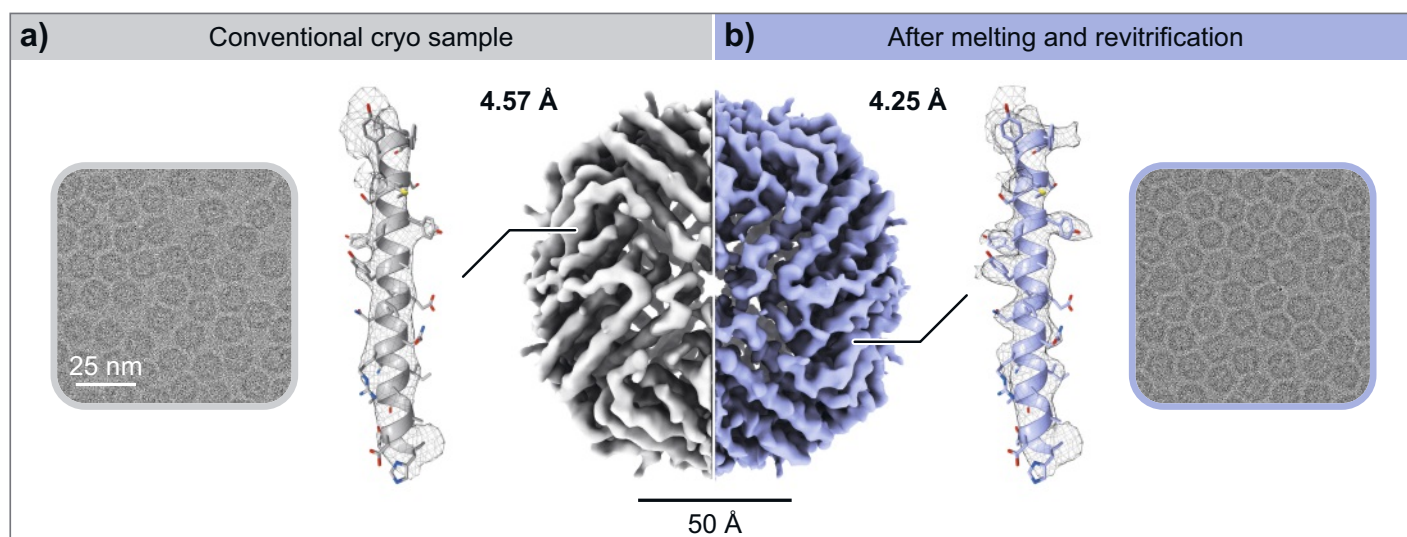
Fig. 7. Melting and revitrification preserves protein structure. (a,b) Micrographs and single-particle reconstructions of apoferritin in a conventional cryo sample (a) and in a sample that has been melted and revitrified (b). The two reconstructions are indistinguishable within the resolution of our instrument, showing that the revitrification process preserves the structure of the protein. The details show the density of an alpha helix that has been fitted with PDB model 6V21.[76] (Adapted from ref. [72].)

the sample is melted, at which point dynamics start to unfold. Finally, we are currently also working on making our technique more broadly accessible. Setting up a time-resolved instrument as we have developed it in our lab presents a significant hurdle for the adoption of our technique. We are therefore currently implementing an *ex situ* revitrification approach that uses an optical microscope. Finally, we hope to demonstrate that our approach can provide novel insights into the fast dynamics of a variety of proteins. We have therefore begun studies of a range of different systems.

Acknowledgments

Competing Interest Statement

The authors declare no competing financial interests.

July 29, 2022

[1] L. Pauling, Nobel Lecture, **1954**, https://www.nobelprize.org/prizes/chemistry/1954/pauling/lecture/.

[2] A. H. Zewail, *Angew. Chem. Int. Ed.* **2000**, *39*, 2586, https://doi.org/10.1002/1521-3773(20000804)39:15<2586::AID-ANIE2586>3.0.CO;2-O.

[3] A. H. Zewail, *Chem. Phys.* **2010**, *378*, 1. https://doi.org/10.1016/j.chemphys.2010.09.008.

[4] P. B. Moore, W. A. Hendrickson, R. Henderson, A. T. Brunger, *Science* **2022**, *375*, 507, https://doi.org/10.1126/science.abn9422.

[5] L. W. Swanson, G. A. Schwind, 'Handbook of Charged Particle Optics', Chap. 1, CRC Press, **2009**.

[6] L. W. Swanson, G. A. Schwind, *Adv. Imaging Electron Phys.* **2009**, *159*, 63, https://doi.org/10.1016/S1076-5670(09)59002-7.

[7] M. S. Bronsgeest, 'Physics of Schottky Electron Sources: Theory and Optimum Operation', Jenny Stanford Publishing, **2014**.

[8] M. T. Otten, W. M. J. Coene, *Ultramicroscopy* **1993**, *48*, 77, https://doi.org/10.1016/0304-3991(93)90173-U.

[9] H. Lichte, M. Lehmann, *Rep. Prog. Phys.* **2008**, *71*, 016102, https://doi.org/10.1088/0034-4885/71/1/016102.

[10] R. S. Ruskin, Z. Yu, N. Grigorieff, *J. Struct. Biol.* **2013**, *184*, 385, https://doi.org/10.1016/j.jsb.2013.10.016.

[11] G. McMullan, A. R. Faruqi, D. Clare, R. Henderson, *Ultramicroscopy* **2014**, *147*, 156, https://doi.org/10.1016/j.ultramic.2014.08.002.

[12] M. Adrian, J. Dubochet, J. Lepault, A. W. McDowall, *Nature* **1984**, *308*, 32, https://doi.org/10.1038/308032a0.

[13] J. Dubochet, M. Adrian, J.-J. Chang, J.-C. Homo, J. Lepault, A. W. McDowall, P. Schultz, *Quart. Rev. Biophys.* **1988**, *21*, 129, https://doi.org/10.1017/s0033583500004297.

[14] W. Kuhlbrandt, *Science* **2014**, *343*, 1443, https://doi.org/10.1126/science.1251652.

[15] E. Hand, *Science* **2020**, *367*, 354, https://doi.org/10.1126/science.367.6476.354.

[16] N. de Jonge, F. M. Ross, *Nat. Nanotechnol.* **2011**, *6*, 695, https://doi.org/10.1038/nnano.2011.161.

[17] Z. Liu, M. A. Monclús, L. W. Yang, M. Castillo-Rodríguez, J. M. Molina-Aldareguía, J. LLorca, *Extreme Mech. Lett.* **2018**, *25*, 60, https://doi.org/10.1016/j.eml.2018.10.007.

[18] D. M. Foster, Th. Pavloudis, J. Kioseoglou, R. E. Palmer, *Nat. Commun.* **2019**, *10*, 2583, https://doi.org/10.1038/s41467-019-10713-z.

[19] B. Westenfelder, J. C. Meyer, J. Biskupek, G. Algara-Siller, L. G. Lechner, J. Kusterer, U. Kaiser, C. E. Krill, E. Kohn, F. Scholz, *J. Phys. D: Appl. Phys.* **2011**, *44*, 055502, https://doi.org/10.1088/0022-3727/44/5/055502.

[20] Z. Zeng, W.-I. Liang, H.-G. Liao, H. L. Xin, Y.-H. Chu, H. Zheng, *Nano Lett.* **2014**, *14*, 1745, https://doi.org/10.1021/nl403922u.

[21] J. M. Voss, P. K. Olshin, R. Charbonnier, M. Drabbels, U. J. Lorenz, *ACS Nano* **2019**, *13*, 12445, https://doi.org/10.1021/acsnano.9b06664.

[22] A. H. Zewail, *Science* **2010**, *328*, 187, https://doi.org/10.1126/science.1166135.

[23] N. D. Browning, M. A. Bonds, G. H. Campbell, J. E. Evans, T. LaGrange, K. L. Jungjohann, D. J. Masiel, J. McKeown, S. Mehraeen, B. W. Reed, M. Santala, *Curr. Opin. Solid State Mater. Sci.* **2012**, *16*, 23, https://doi.org/10.1016/j.cossms.2011.07.001.

[24] A. Feist, N. Bach, N. Rubiano da Silva, T. Danz, M. Möller, K. E. Priebe, T. Domröse, J. G. Gatzmann, S. Rost, J. Schauss, S. Strauch, R. Bormann, M. Sivis, S. Schäfer, C. Ropers, *Ultramicroscopy* **2017**, *176*, 63, https://doi.org/10.1016/j.ultramic.2016.12.005.

[25] M. Picher, K. Bücker, T. LaGrange, F. Banhart, *Ultramicroscopy* **2018**, *188*, 41, https://doi.org/10.1016/j.ultramic.2018.03.006.

[26] P. K. Olshin, M. Drabbels, U. J. Lorenz, *Struct. Dyn.* **2020**, *7*, 054304, https://doi.org/10.1063/4.0000034.

[27] A. R. Ziefuss, S. Reich, S. Reichenberger, M. Levantino, A. Plech, *Phys. Chem. Chem. Phys.* **2020**, *22*, 4993, https://doi.org/10.1039/C9CP05202J.

[28] T. Katayama, K. Setoura, D. Werner, H. Miyasaka, S. Hashimoto, *Langmuir* **2014**, *30*, 9504, https://doi.org/10.1021/la500663x.

[29] L. Delfour, T. E. Itina, *J. Phys. Chem. C* **2015**, *119*, 13893, https://doi.org/10.1021/acs.jpcc.5b02084.

[30] K. Saha, S. S. Agasti, C. Kim, X. Li, V. M. Rotello, *Chem. Rev.* **2012**, *112*, 2739, https://doi.org/10.1021/cr2001178.

[31] P. D. Howes, R. Chandrawati, M. M. Stevens, *Science* **2014**, *346*, 1247390, https://doi.org/10.1126/science.1247390.

[32] J. Oliver-Meseguer, M. Boronat, A. Vidal-Moya, P. Concepción, M. Á. Rivero-Crespo, A. Leyva-Pérez, A. Corma, *J. Am. Chem. Soc.* **2018**, *140*, 3215, https://doi.org/10.1021/jacs.7b13696.

[33] X. Huang, I. H. El-Sayed, W. Qian, M. A. El-Sayed, *J. Am. Chem. Soc.* **2006**, *128*, 2115, https://doi.org/10.1021/ja057254a.

[34] S. D. Brown, P. Nativo, J.-A. Smith, D. Stirling, P. R. Edwards, B. Venugopal, D. J. Flint, J. A. Plumb, D. Graham, N. J. Wheate, *J. Am. Chem. Soc.* **2010**, *132*, 4678, https://doi.org/10.1021/ja908117a.

[35] H. A. Atwater, A. Polman, *Nat. Mater.* **2010**, *9*, 205, https://doi.org/10.1038/nmat2629.

[36] Y. H. Jang, Y. J. Jang, S. Kim, L. N. Quan, K. Chung, D. H. Kim, *Chem. Rev.* **2016**, *116*, 14982, https://doi.org/10.1021/acs.chemrev.6b00302.

[37] S. Hashimoto, D. Werner, T. Uwada, *J. Photochem. Photobiol. C* **2012**, *13*, 28, https://doi.org/10.1016/j.jphotochemrev.2012.01.001.

[38] G. González-Rubio, A. Guerrero-Martínez, L. M. Liz-Marzán, *Acc. Chem. Res.* **2016**, *49*, 678, https://doi.org/10.1021/acs.accounts.6b00041.

[39] D. Werner, A. Furube, T. Okamoto, S. Hashimoto, *J. Phys. Chem. C* **2011**, *115*, 8503, https://doi.org/10.1021/jp112262u.

[40] S. Besner, A. V. Kabashin, M. Meunier, *Appl. Phys. A* **2007**, *88*, 269, https://doi.org/10.1007/s00339-007-4001-1.

[41] S. Inasawa, M. Sugiyama, Y. Yamaguchi, *J. Phys. Chem. B* **2005**, *109*, 9404, https://doi.org/10.1021/jp0441240.

[42] A. Plech, V. Kotaidis, M. Lorenc, J. Boneberg, *Nat. Phys.* **2006**, *2*, 44, https://doi.org/10.1038/nphys191.

[43] Y. Ihm, D. H. Cho, D. Sung, D. Nam, C. Jung, T. Sato, S. Kim, J. Park, S. Kim, M. Gallagher-Jones, Y. Kim, R. Xu, S. Owada, J. H. Shim, K. Tono, M. Yabashi, T. Ishikawa, J. Miao, D. Y. Noh, C. Song, *Nat. Commun.* **2019**, *10*, 2411, https://doi.org/10.1038/s41467-019-10328-4.

[44] G. Bongiovanni, P. K. Olshin, C. Yan, J. M. Voss, M. Drabbels, U. J. Lorenz, *Nanoscale Adv.* **2021**, *3*, 5277, https://doi.org/10.1039/D1NA00406A.

[45] E. A. Ring, N. de Jonge, *Microsc. Microanal.* **2010**, *16*, 622, https://doi.org/10.1017/S1431927610093669.

[46] M. R. Langille, M. L. Personick, C. A. Mirkin, *Angew. Chem. Int. Ed.* **2013**, *52*, 13910, https://doi.org/10.1002/anie.201301875.

[47] Y. Zhai, J. S. DuChene, Y.-C. Wang, J. Qiu, A. C. Johnston-Peck, B. You, W. Guo, B. DiCiaccio, K. Qian, E. W. Zhao, F. Ooi, D. Hu, D. Su, E. A. Stach, Z. Zhu, W. D. Wei, *Nat. Mater.* **2016**, *15*, 889, https://doi.org/10.1038/nmat4683.

[48] J. E. Evans, N. D. Browning, *Microscopy (Tokyo)* **2013**, *62*, 147, https://doi.org/10.1093/jmicro/dfs081.

[49] L. Zhang, J. P. Hoogenboom, B. Cook, P. Kruit, *Struct. Dyn.* **2019**, *6*, 051501, https://doi.org/10.1063/1.5117058.

[50] G. Bongiovanni, P. K. Olshin, M. Drabbels, U. J. Lorenz, *Appl. Phys. Lett.* **2020**, *116*, 234103, https://doi.org/10.1063/5.0009442.

[51] P. K. Olshin, G. Bongiovanni, M. Drabbels, U. J. Lorenz, *Nano Lett.* **2021**, *21*, 612, https://doi.org/10.1021/acs.nanolett.0c04184.

[52] A. H. V. van Veen, C. W. Hagen, J. E. Barth, P. Kruit, *J. Vac. Sci. Technol. B* **200**1, *19*, 2038, https://doi.org/10.1116/1.1409390.

[53] B. Cook, T. Verduin, C. W. Hagen, P. Kruit, *J. Vac. Sci. Technol. B* **2010**, *28*, C6C74, https://doi.org/10.1116/1.3502642.

[54] L. Protesescu, S. Yakunin, M. I. Bodnarchuk, F. Krieg, R. Caputo, C. H. Hendon, R. X. Yang, A. Walsh, M. V. Kovalenko, *Nano Lett.* **2015**, *15*, 3692, https://doi.org/10.1021/nl5048779.

[55] Q. A. Akkerman, G. Rainò, M. V. Kovalenko, L. Manna, *Nat. Mater.* **2018**, *17*, 394, https://doi.org/10.1038/s41563-018-0018-4.

[56] M. Liao, B. Shan, M. Li, *J. Phys. Chem. Lett.* **2019**, *10*, 1217, https://doi.org/10.1021/acs.jpclett.9b00344.

[57] J. Frank, 'Conformational Proteomics of Macromolecular Architecture: Approaching the Structure of Large Molecular Assemblies and Their Mechanisms of Action', Chap. 13, World Scientific, **2004**.

[58] J. Frank, 'Three-Dimensional Electron Microscopy of Macromolecular Assemblies: Visualization of Biological Molecules in Their Native State', Oxford University Press, **2006**.

[59] E. Cao, M. Liao, Y. Cheng, D. Julius, *Nature* **2013**, *504*, 113, https://doi.org/10.1038/nature12823.

[60] J. Zhao, S. Benlekbir, J. L. Rubinstein, *Nature* **2015**, *521*, 241, https://doi.org/10.1038/nature14365.

[61] K. Henzler-Wildman, D. Kern, *Nature* **2007**, *450*, 964, https://doi.org/10.1038/nature06522.

[62] D. D. Boehr, H. J. Dyson, P. E. Wright, *Chem. Rev.* **2006**, *106*, 3055, https://doi.org/10.1021/cr050312q.

[63] Y. Shi, *Cell* **2014**, *159*, 995, https://doi.org/10.1016/j.cell.2014.10.051.

[64] F. Schotte, M. Lim, T. A. Jackson, A. V. Smirnov, J. Soman, J. S. Olson, G. N. Jr. Phillips, M. Wulff, P. A. Anfinrud, *Science* **2003**, *300*, 1944, https://doi.org/10.1126/science.1078797.

[65] K. Pande, C. D. M. Hutchison, G. Groenhof, A. Aquila, J. S. Robinson, J. Tenboer, S. Basu, S. Boutet, D. P. DePonte, M. Liang, T. A. White, N. A. Zatsepin, O. Yefanov, D. Morozov, D. Oberthuer, C. Gati, G. Subramanian, D. James, Y. Zhao, J. Koralek, J. Brayshaw, C. Kupitz, C. Conrad, S. Roy-Chowdhury, J. D. Coe, M. Metz, P. L. Xavier, T. D. Grant, J. E. Koglin, G. Ketawala, R. Fromme, V. rajer, R. Henning, J. C. H. Spence, A. Ourmazd, P. Schwander, U. Weierstall, M. Frank, P. Fromme, A. Barty, H. N. Chapman, K. Moffat, J. J. van Thor, M. Schmidt, *Science* **2016**, *352*, 725, https://doi.org/10.1126/science.aad5081.

[66] J. Berriman, N. Unwin, *Ultramicroscopy* **1994**, *56*, 241, https://doi.org/10.1016/0304-3991(94)90012-4.

[67] N. Unwin, Y. Fujiyoshi, *J. Mol. Biol.* **2012**, *422*, 617, https://doi.org/10.1016/j.jmb.2012.07.010.

[68] B. Chen, J. Frank, *Microscopy* **2016**, *65*, 69, https://doi.org/10.1093/jmicro/dfv344.

[69] J. Frank, *J. Struct. Biol.* **2017**, *200*, 303, https://doi.org/10.1016/j.jsb.2017.06.005.

[70] J. M. Voss, O. F. Harder, P. K. Olshin, M. Drabbels, U. J. Lorenz, *Chem. Phys. Lett.* **2021**, *778*, 138812, https://doi.org/10.1016/j.cplett.2021.138812.

[71] J. M. Voss, O. F. Harder, P. K. Olshin, M. Drabbels, U. J. Lorenz, *Struct. Dyn.* **2021**, *8*, 054302, https://doi.org/10.1063/4.0000129.

[72] O. F. Harder, J. M. Voss, P. K. Olshin, M. Drabbels, U. J. Lorenz, *Acta Crystallogr. D* **2022**, *78*, 883, https://doi.org/10.1107/s205979832200554x.

[73] G. C. R. Ellis-Davies, *Nat. Methods* **2007**, *4*, 619, https://doi.org/10.1038/nmeth1072.

[74] Y. Shigeri, Y. Tatsu, N. Yumoto, *Pharmacol. Ther.* **2001**, *91*, 85, https://doi.org/10.1016/s0163-7258(01)00148-6.

[75] C. J. Russo, L. A. Passmore, *Science* **2014**, *346*, 1377, https://doi.org/10.1126/science.1259530.

[76] M. Wu, G. C. Lander, M. A. Herzik Jr., *J. Struct. Biol.: X* **2020**, *4*, 100020, https://doi.org/10.1016/j.yjsbx.2020.100020.

[77] A. Tirla, P. Rivera-Fuentes, *Angew. Chem. Int. Ed.* **2016**, *55*, 14709, https://doi.org/10.1002/anie.201608779.

[78] M. Gutman, 'Methods of Biochemical Analysis', Chap. 1, John Wiley & Sons, Inc., **1984**.

[79] K. Suyama, M. Shirai, *Prog. Polym. Sci.* **2009**, *34*, 194, https://doi.org/10.1016/j.progpolymsci.2008.08.005.